Arabian Journal of Chemistry (2011) **4**, 449–457

King Saud University

Arabian Journal of Chemistry

www.ksu.edu.sa
www.sciencedirect.com

ORIGINAL ARTICLE

Influence of acid–base properties of cobalt–molybdenum catalysts supported on magnesium orthophosphates in isomerization of 3,3-dimethylbut-1-ene

M. Sadiq [a], A. Sahibed-dine [a], M. Baalala [a], K. Nohair [a], M. Abdennouri [a], M. Bensitel [a,*], C. Lamonier [b], J. Leglise [c]

[a] *Laboratoire de Catalyse et Corrosion des Matériaux, Université Chouaib Doukkali, Faculté des Sciences d'El Jadida, BP. 20, El Jadida 24000, Morocco*
[b] *Unité de Catalyse et Chimie du solide, LCH, bât C3, UMR8181, 59650 Villeneuve d'Ascq, Lille, France*
[c] *DRRT, 2 rue Grenet Tellier, 51038 Châlons en Champagne, France*

Received 25 March 2010; accepted 5 June 2010
Available online 17 July 2010

KEYWORDS

Magnesium phosphates (MgP);
Co–Mo/MgP;
Structural and textural properties;
3,3-Dimethylbut-1-ene isomerization

Abstract Synthesis and physico-chemical characterization of a pure magnesium phosphate (MgP) prepared by coprecipitation, and MgP modified by introduction of cobalt–molybdenum (4–12 wt.% of MoO_3 with the Co/Mo ratio fixed at 0.5) have been carried out. The structural properties of these catalysts were characterized by X-ray diffraction, their textural properties were determined by N_2 adsorption–desorption isotherms and the dispersion of cobalt–molybdenum was studied by XPS spectroscopy. Their acid properties have been investigated by in situ FT-IR spectroscopy of adsorbed molecules, often, 2,6-dimethylpyridine (pK_a = 6.7), pyridine (pK_a = 5.3). Co–Mo incorporation leads to a modification in the MgP acid–base properties, especially on the acid sites type and number. Thus, lower loading of cobalt–molybdenum species decreased the number of strong Lewis acid sites whereas higher loading increased it. It was found that Lewis acid sites on magnesium phosphates play an important role in the isomerization of 3,3-dimethylbut-1-ene.

* Corresponding author. Tel.: +212 23343003; fax: +212 23342187.
E-mail addresses: sadiqmhamed@hotmail.com (M. Sadiq), mbensitel@yahoo.fr (M. Bensitel).

Peer-review under responsibility of King Saud University.
doi:10.1016/j.arabjc.2010.07.015

Production and hosting by Elsevier

The 3,3-dimethylbut-1-ene (33DMB1) conversion increases with the reaction temperature from 493 to 653 K for MgP, but decreases after 573 K for MgP supported by Co–Mo. A linear relationship between both types of acid sites and conversion values was found. The deactivation of the catalysts appears at high reaction temperature (> 573 K).

1. Introduction

Acidic solids derived from metal orthophosphates are widely used to catalyse various reactions occurring at the gas/solid interface. Acid–base properties and redox properties are amongst important types of surface chemical properties of metal orthophosphates catalysts. The textural and acid–base properties of the catalysts depend on preparation method, concentration of promoting elements; source of phosphate ion and treatment temperature (Samantaray and Parida, 2001; Sadiq et al., 2008). The acidity of the sites can be determined by an IR spectroscopy estimation of the isosteric heat of adsorption on each type of site (Paukshtis and Yurchenko, 1983; Beebe et al., 1984). Lutidine and pyridine have been chosen as an IR probe because with the adsorption of these basic molecules, surface acid properties of solids can be determined at room and at higher temperature in relation to the adsorption strength.

The OH-groups are formed as a result of dissociative adsorption of H_2O molecules, which occurs in order to reduce the coordinative unsaturation of the surface sites (Boehm and Knözinger, 1983). Surface OH-groups are sensitive intrinsic probes for the surface structure (Boehm and Knözinger, 1983; Zaki and Knozinger, 1987). A number of metal phosphates have been used as heterogeneous catalysts for various organic processes in recent years, amongst them, skeletal isomerisation of 1,3 dimethyl-1-butene, 2,3-dimethyl-2-butene and 3,3-(dimethtl) dimethyl-1-butene (Gallace and Moffat, 1982). Aramendia et al. (2000) studied the effect of Na_2CO_3 impregnation on the activity of $Mg_3(PO_4)_2$ in the dehydration 2-hexanol, and shown that the acidity of $Mg_3(PO_4)_2$ decreases after addition of Na_2CO_3. Others authors have examined the density effect of Brônsted and Lewis acid sites of $CoMo/AlPO_4$ catalysts, on the activity of 2-butanol dehydration (Rouimi et al., 1999). Sokolovski et al. (1993) studied the oxidative transformation of methane on magnesium–phosphorus catalyst and proved the acidity resulting from P on selectivity from dimerisation to oxidation. The acid and basic surface properties of metallic phosphates solids are modified by addition of urea, alkaline ions (Campelo et al., 1983), and fluoride or sulphate anions (Campelo et al., 1984). Aramendia et al. (2002) have studied an influence of the composition of magnesium phosphate catalysts on the transformation of 2-hexanol. The dehydration–dehydrogenation of alcohols is a model reaction for the acid–base properties of these solid catalysts (Aramendia et al., 1996). The presence of MoO_3 has a synergistic effect on $BiPO_4$ in the dehydration of amides (Tascon et al., 1986).

The 33DMB1 skeletal isomerisation has been studied on various metal oxides (Martin and Duprez, 1997; Haneda et al., 2001) and phosphates (Gallace and Moffat, 1982; Florentino et al., 1992; Bautista et al., 1998) and thus, it becomes a model reaction with a mechanism involving secondary carbenium ions on Brônsted sites (Martin and Duprez, 1997; Haneda et al., 2001; Guisnet, 1990).

The skeletal isomerisation of 3,3-dimethylbut-1-ene (33DMB1) with the reaction scheme (Fig. 1), is relatively simple with only two main products: 2,3-dimethylbut-1-ene (23DMB1) and 2,3-dimethylbut-2-ene (23DMB2). Other weaker products appear at higher temperatures (> 573 K). These products are attributed to methylpentenes (Irvine et al., 1980). The slow step of the reaction is probably the isomerisation of the carbocation intermediate through the methyl group migration.

In the present work, we demonstrate and discuss in situ the FT-IR spectra of pyridine and 2,6-dimethylpyridine (lutidine) on pure and supported MgP at temperature $\geqslant$ RT, for the identification of acid sites exposed on the surface of our catalysts. The textural characterisations have been determined by N_2 adsorption–desorption isotherms. The bulk and surface properties of the catalysts characterised by X-ray powder diffractometry and photoelectron spectroscopy, and the 33DMB1 skeletal isomerisation has been studied on pure and supported MgP in order to understand the correlation with the surface acid properties.

2. Experimental

2.1. Catalysts synthesis

Magnesium orthophosphates were synthesised using the following procedure: a solution containing 40 g of $Mg(NO_3)_2{\cdot}6H_2O$ and 7.08 ml of 85% H_3PO_4 in 100 ml of distiled water is prepared and placed in an ice bath. It is then slowly supplied dropwise with a NaOH (0.4 N) solution under stirring, up to pH 9. The obtained gel is kept for 24 h under ambient conditions. It is then filtered, and air-dried at 353 K. The solid is then calcined at 773 K during 3 h and sifted through 0.2–0.5 mm.

A series of cobalt–molybdenum catalysts CoMo1/MgP, CoMo2/MgP and CoMo3/MgP were prepared using successive impregnation method, over an MgP support. A mass of ammonium heptamolybdate $[(NH_4)_6Mo_7O_{24}{\cdot}4H_2O]$ calculated to yield the desired percentage of molybdenum on the support, was dissolved in a predetermined volume of distiled water. This volume calculation is based on the pore volume of the support. The pH solution is adjusted at 7 with addition of NH_4OH solution.

The impregnated catalysts Mo/MgP were dried at 383 K for 12 h and calcined under air flow at 673 K during 4 h. A second impregnation over Mo/MgP by an aqueous solution of cobalt nitrate $[Co(NO_3)_2{\cdot}6H_2O]$, in order to obtain a Co/Mo ratio equal to 0.5, is done. Finally, the impregnated catalysts are dried at 383 K during 12 h and calcined under air flow at 673 K for 4 h. The nomenclature of the catalysts with the loading in wt.% of molybdenum and cobalt is given in Table 1. Another catalyst (CoMo22/MgP) was prepared by depositing both the Co and Mo species simultaneously. For comparison

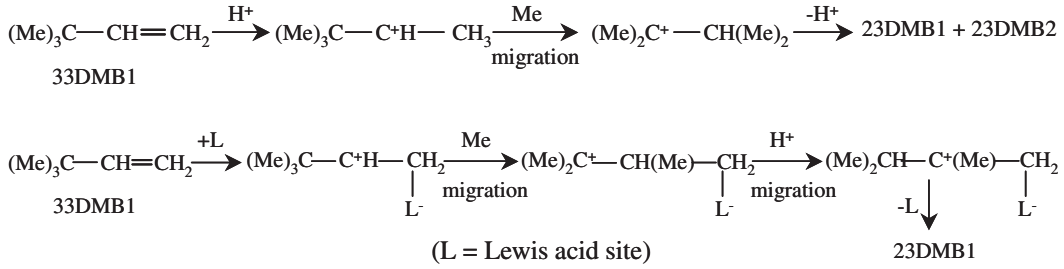

Figure 1 3,3-Dimethylbut-1-ene (33DMBl) isomerization scheme, according to Irvine et al. (1980).

Table 1 Nomenclature and metal loading of the catalyst expressed as Mo (or MoO_3) and Co (or CoO) wt%.

Nomenclature	Mo% (g/g cat)	Co% (g/g cat)	MoO_3% (g/g cat)	CoO% (g/g cat)
CoMo1/MgP	2.71	0.82	4.06	1.04
Mo2/MgP	5.31	–	8.00	–
Co2/MgP	–	1.66	–	2.18
CoMo2/MgP or CoMo22/MgP	5.23	1.58	7.84	2.01
CoMo3/MgP	7.70	2.33	11.55	2.96

purposes, reference samples Mo2/MgP and Co2/MgP have been synthesised as also those of CoMo2/MgP.

2.2. Characterization of the synthesized solids

2.2.1. X-ray diffraction analysis

X-ray diffraction (XRD) patterns were recorded on a Siemens D5000 diffractometer using Cu Kα radiation. The patterns are collected at 298 K and recorded with a step of 0.04° using a counting time of 1 s/step over the 2θ range from 3 to 80.

2.2.2. Textural properties of the solids

The specific surface area, pore volume and pore diameter were measured from nitrogen adsorption–desorption isotherms recorded on a Micromeritics ASAP-2000 instruments. The BET method and BJH method are, respectively, used to calculate specific surface area and pore distributions; all the samples were degassed at 673 K before measurements.

2.2.3. In situ FT-IR spectroscopy

Self-supporting wafers ($10 \pm 2\ mg\ cm^{-2}$) of the adsorbents were prepared and mounted inside a specially designed cell; they were heated and activated under vacuum at different temperatures before the addition of probe molecules. The cell was evacuated to $\sim 10^{-5}$ torr at RT, then by another evacuation at 673 K for 2 h. Subsequently, the wafer was cooled under vacuum ($\sim 10^{-5}$ torr) to RT, before being adsorbed by the probe molecules. The cell and wafer background (BKg) spectra were taken over the frequency range 4000–400 cm^{-1} with a resolution of 4 cm^{-1} using a model Nicolet 710 FT-IR spectrometer.

2.2.4. X-ray photoelectron spectroscopy (XPS)

The X-ray photoelectron spectroscopy analyses were performed with an EscaLab 220-IXL (VG Scientific), equipped with a dual Mg/Al anode. The spectra were excited by the monochromatised Al Kα source (1486.6 eV). The pressure in the analysis chamber was in the range of 10^{-10} torr during data collection. The constant charging of the samples was removed by referencing all the energies to the C 1s peak energy at 285 eV.

2.2.5. Catalytic test

Isomerisation of 3,3-dimethylbut-1-ene (33DMB1) was carried out in a fixed-bed type reactor with a continuous flow system at atmospheric pressure. The reactant, 33DMB1 (21.2 kPa), was diluted in nitrogen by bubbling the gas through the liquid reactant in a saturator maintained at 273 K. The 33DMB1 isomerisation was performed at a temperature between 493 and 653 K. The products were analysed by on-line gas chromatography (FID) using a capillary Squalane column (100 m, 0.26 mm id) maintained at 313 K.

The rate constant ($mmol\ h^{-1}\ g^{-1}\ bar^{-1}$) was calculated after each analysis by the form:

$$K(T) = -\ln(1 - X)\frac{F_0}{P^0 W}$$

where X is the conversion, P^0 the pressure, F_0 the molar flow rate of 33DMB1 and W (60 mg) the catalyst weight.

3. Results and discussion

3.1. Characterization of solids

3.1.1. XRD patterns

In a previous work we studied by XRD analysis the crystalline evolution of the MgP support during calcination (Sadiq et al., 2005). A comparison of the peaks observed with those listed in JCPDS files allowed an identification of the solids by their structure. The dried solid MgP at 353 K consisted of $Mg_3(PO_4)_2{\cdot}5H_2O$ (JCPDS 35-0329) and also, some weaker diffraction stripes have been assigned to $Mg_3(PO_4)_2{\cdot}8H_2O$ (JCPDS 33-0877). This solid became amorphous after calcination at 773 K. At 973 K, it is converted into the crystalline phase $Mg_3(PO_4)_2$ (JCPDS 75-1491) (Fig. 2).

The solids impregnated with Co–Mo have been also studied. They also became amorphous after calcination at 773 K. Their patterns are similar to those of MgP solid. However the calcination at 973 K of these solids lead not only to the previous phase identified for $Mg_3(PO_4)_2$ [JCPDS 75-1491] but also

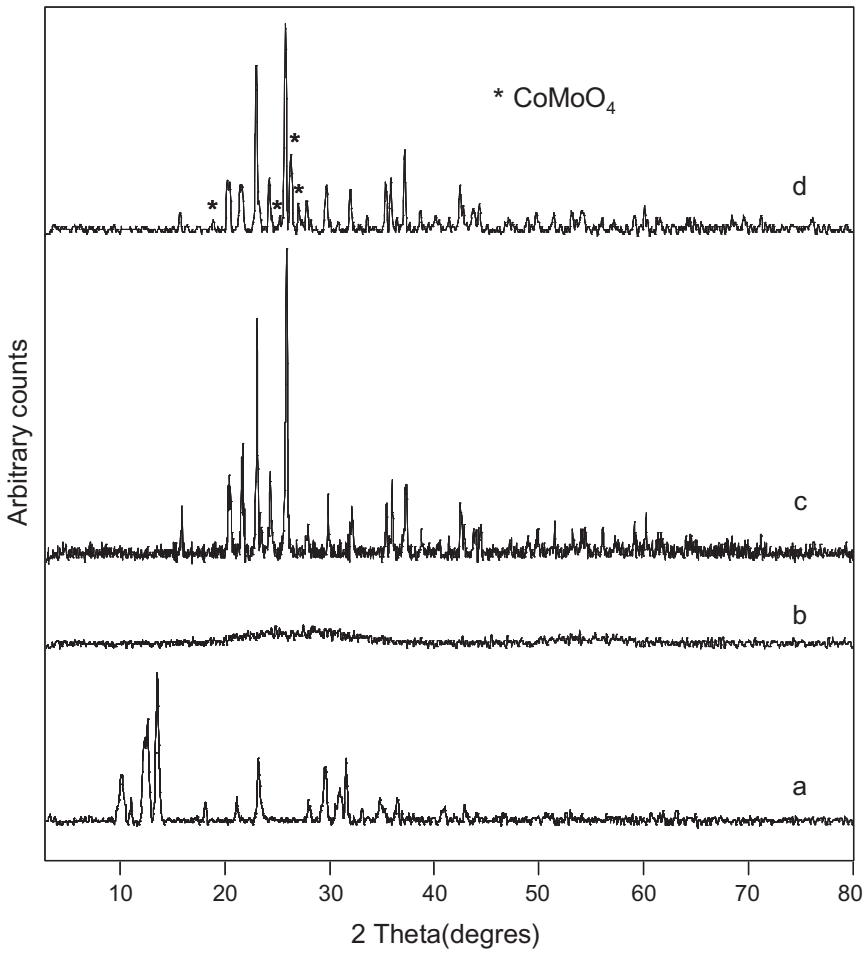

Figure 2 XRD patterns for solids MgP calcined at 353 K (a), 773 K (b), 973 K (c) and CoMo2/MgP calcined at 973 K (d).

to a new crystalline phase $CoMoO_4$ [JCPDS 21-0868] (Fig. 2d). This suggested that Co–Mo is well dispersed over the surface of the phosphate.

3.1.2. Textural properties of the calcined solids

Fig. 3 shows the N_2 adsorption–desorption isotherms and Table 2 the specific surface area (S_{BET}), cumulative pore volume (V_p at $P/P° = 0.98$), and average pore diameter for the synthesised solids. All the solids exhibit a type IV isotherm according to the Brunauer–Deming–Deming–Teller classification (Brunauer et al., 1940), the hysteresis loop can be observed in all solids, as an intermediate between types H1 and H3, which are associated with materials possessing open-end cylindrical pores and exhibit no limiting adsorption at high P/P_0 ratios, that is observed with aggregates of plate-like particles giving rise to slit-shaped pores, respectively (Sing et al., 1985). The average pore diameter for these solids is classed in the mesoporous range, according to Sing et al. (1985).

However, an increasing of the Co–Mo content in the samples decreases specific surface area and pore volume (Table 2), the same effect has been observed with the deposition of sodium carbonate on magnesium orthophosphates (Aramendia et al., 1999). That is probably due to the reduction of the porous volume concentration or to the pores replenishments.

3.2. FT-IR spectroscopy of adsorbed pyridine and lutidine

3.2.1. Hydroxyl groups (region 3750–3000 cm^{-1})

The spectra in the ν_{OH} (OH stretching) region of the catalysts after 2 h outgassing at 673 K under vacuum show only one sharp band at 3676 cm^{-1} (for example MgP support, Fig. 4). This band could be assigned in agreement with Aramendia et al. (1999) to stretching vibrations of OH in P–OH-groups not perturbed by H-bonding hydroxyls.

The location on the surface of the free hydroxyls responsible for this band is confirmed by its decreasing upon adsorption of pyridine or lutidine and outgassing at room temperature for 2 h with the weak increase of the broad band intensity, centred at 3550 cm^{-1}, due to associated OH-groups. During evacuation at higher temperatures a progressive desorption of the pyridine or lutidine is observed, restoring the OH band of free hydroxyls groups, compared with those observed on MgP (Fig. 4) before pyridine is adsorbed. This same behaviour was obtained in CoMo/MgP catalysts. The hydroxyl groups on phosphorus found on the catalyst surface should be responsible for the Brônsted acidity.

3.2.2. Pyridine adsorption (region 1700–1400 cm^{-1})

The IR spectra taken from Py/MgP (Fig. 5) and from Py/catalysts at 373 K (Fig. 6) display absorption bands about 1612, 1577, 1493 and 1448 cm^{-1}. According to the reference data

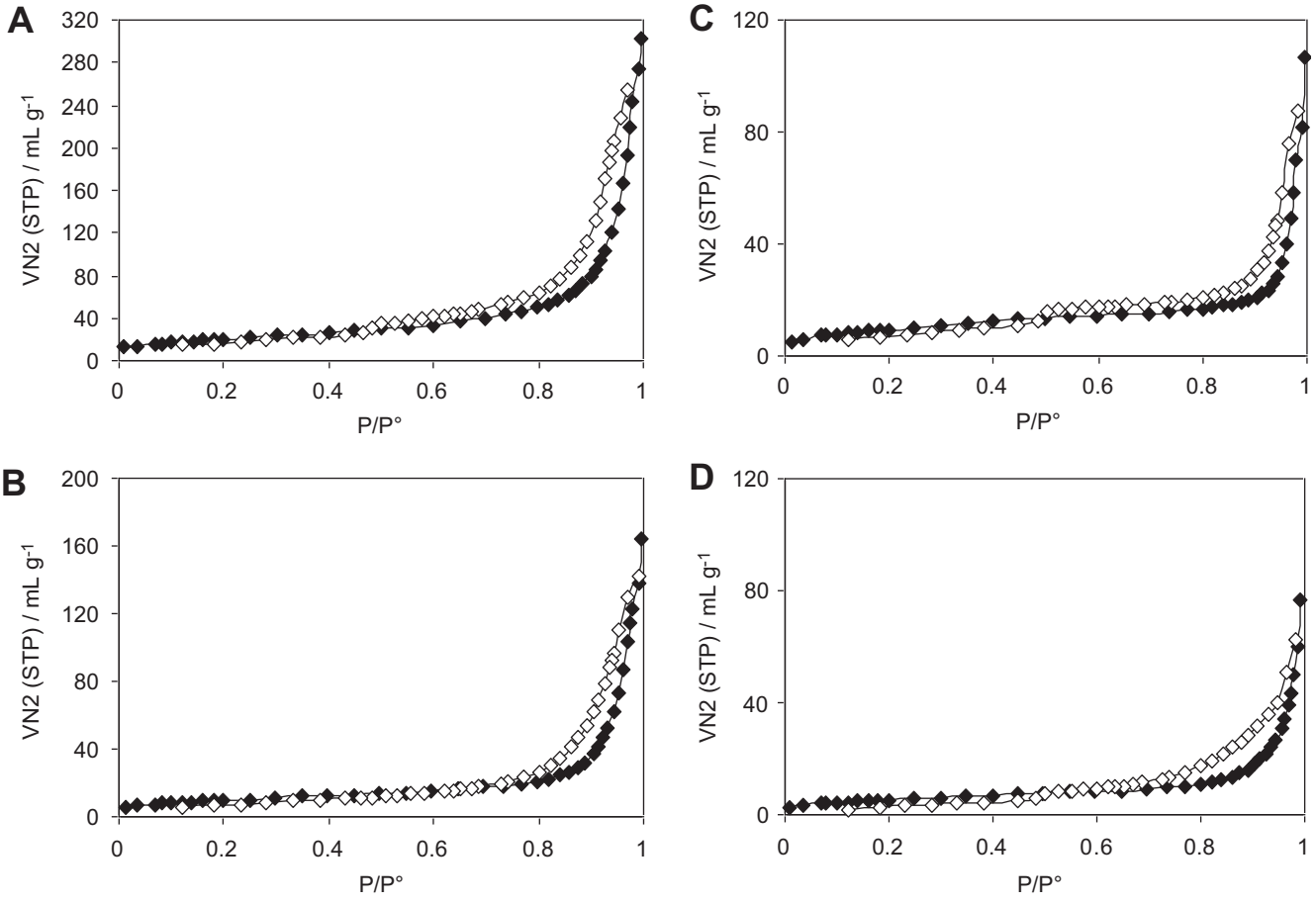

Figure 3 N_2 isotherm showing the adsorption (—◆—) and desorption (—◇—) branches for MgP(A) calcined at 773 K and CoMo1/MgP(B), CoMo2/MgP(C), CoMo3/MgP(D) calcined at 673 K.

Table 2 Specific surface area (S_{BET}), cumulative pore volume (V_p), and average pore diameter (d_p) for the synthesised solids.

Catalysts	S_{BET} ($m^2\ g^{-1}$)	V_p ($cm^3\ g^{-1}$)	d_p (nm)
MgP	73.84	0.37	20.37
CoMo1/MgP	35.56	0.18	21.24
CoMo2/MgP	35.59	0.10	12.08
CoMo3/MgP	19.61	0.07	15.55

compiled in (Zaki et al., 2000), the bands at 1612 (ν_{8a}) and 1448 cm^{-1} (ν_{19b}) are due to strong Lewis acid sites (LPy species), the band at 1577 cm^{-1} (ν_{8b}) is due to LPy and HPy (OH-bonded Py molecules) whereas the band centred at 1493 cm^{-1} (ν_{19a}) is due to coordinately bonded pyridine and hydrogen bonded pyridine. Moreover, FT-IR spectra reveal a band about 1646 cm^{-1}, due to protonated pyridine according to literature (Campelo et al., 1995). After outgassing at higher temperature the band intensities are reduced significantly and shifted to lower frequency values as shown in Fig. 5. This is indicative of an increase in the strength of acidic sites. Generally, the ν_{8a} wavenumber allows one to determine the Lewis acid site strength, whereas the band intensity characterises their number. As seen in Figs. 6 and 7, the number of Lewis acid sites decreases when the Co–Mo loading increases, but this number regenerated for the CoMo3/MgP catalyst that

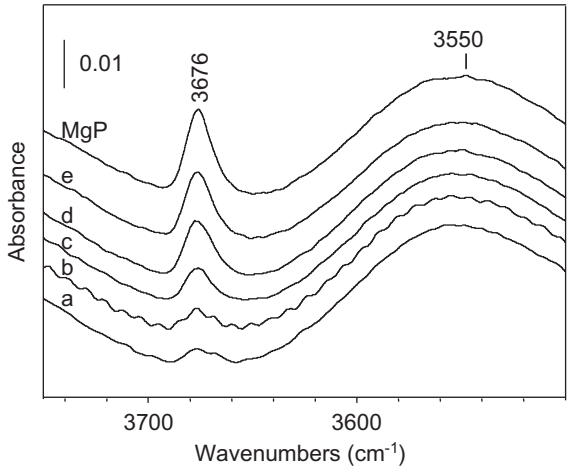

Figure 4 FT-IR spectra (OH stretching) of pyridine adsorbed on MgP support. (MgP) originally after outgassing at 673 K for 2 h, after exposure to pyridine and outgassing, (a) RT, (b) 323 K, (c) 373 K, (d) 423 K and (e) 473 K.

contains a high Co–Mo load. This indicates that our pure MgP support possesses a high total acidity amount, that Mg or P atoms should be responsible for Lewis acidity in agree-

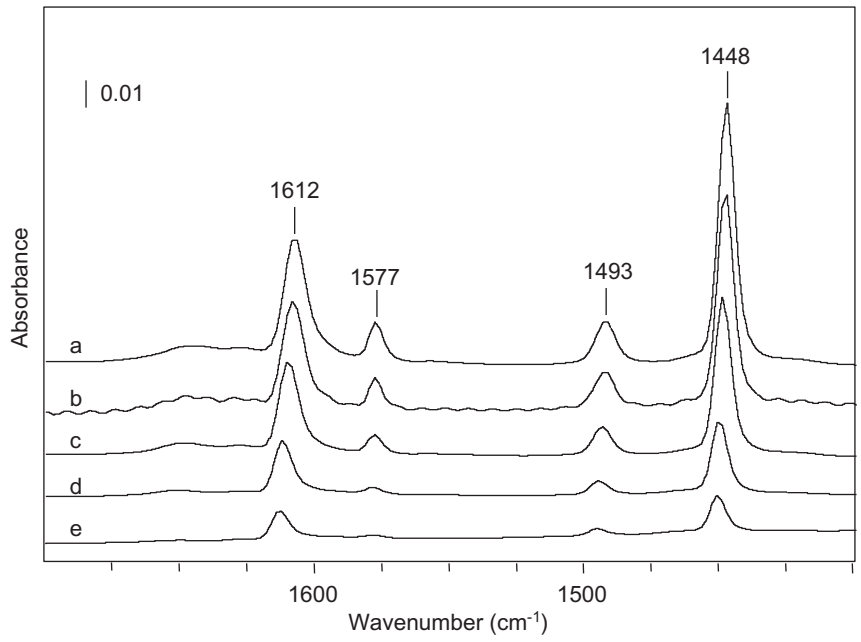

Figure 5 FT-IR spectra of pyridine desorbed at different evacuation temperature (a) RT, (b) 323 (c) 373, (d) 423, and (e) 473 K on MgP.

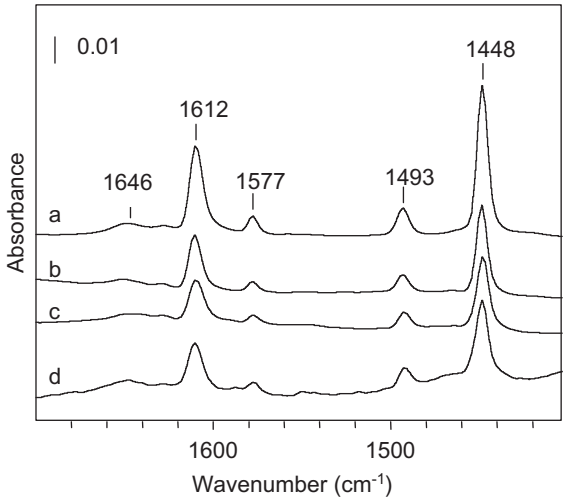

Figure 6 IR spectra of pyridine desorbed at 373 K on: (a) MgP, (b) CoMo1/MgP, (c) CoMo2/MgP, and (d) CoMo3/MgP.

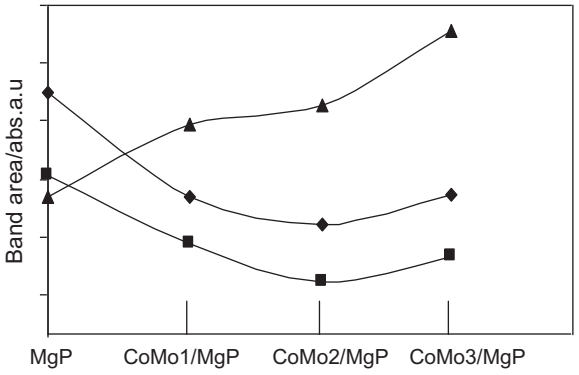

Figure 7 Variation with the catalyst's molybdenum content, of the area of bands characteristic of: (♦) the total number of Lewis (1448 cm^{-1}, pyridine); (■) the strongest Lewis (1612 cm^{-1}, pyridine) and (▲) the Brönsted acid sites (1650 + 1628 cm^{-1}, lutidine) at 373 K.

ment with various authors (Moffat et al., 1985; Zhidomirov and Kazansky, 1986).

3.2.3. Lutidine adsorption (region 1700–1400 cm^{-1})

2,6-Dimethylpyridine (lutidine) is a probe molecule specific to Brônsted acidity, it exhibits a higher basicity (pK_a is 6.7) than pyridine (pK_a is 5.3) (Matulewicz et al., 1980; Corma et al., 1984). For example, Lahousse et al. (1993, 1995) have titrated the Brônsted acid sites of pure and mixed oxides by lutidine, and found that when lutidine is adsorbed on pure and supported MgP activated at 673 K under pumping, a large number of bands arise besides the hydroxyl groups perturbation. Spectra IR (Figs. 8 and 9) after outgassing at higher temperatures show the distinct bands of about 1650, 1628, 1614 and 1583 cm^{-1}. These bands correspond to the ν_{8a} and ν_{8b} modes. Two bands at 1614 and 1583 cm^{-1} remain after heating in vacuum up 470 K, and could be attributed to ν_{8a} and ν_{8b} modes of molecule bound to surface cations by coordinate bond. The bands arise from lutidine adsorption at 1650 and 1628 cm^{-1} and disappear after pumping at 420 K. They correspond to ν_{8a} and ν_{8b} modes of protonated DMP (Petit and Maugé, 1997). Some differences can be noted after impregnation of MgP concerning the frequencies and intensities of the bands, The ν_8 frequencies of $DMPH^+$ and coordinated DMP species bands were shifted to lower wavenumbers when the Co–Mo loading increases. This is related to the higher acidic strength of acid sites of pure MgP than those of MgP supported. More over, the relative intensity of two bands $DMPH^+$ increases with Co–Mo loading, similar results have been reported previously by Martin et al. (1994). They have found MoO_x additives to generate Bronsted acidity on titania surfaces. But those of

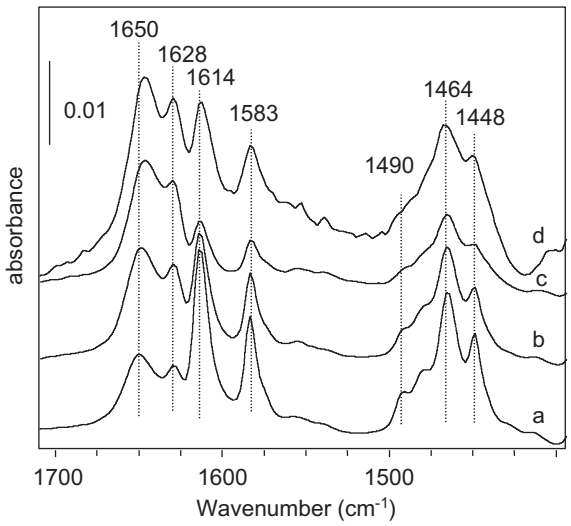

Figure 8 IR spectra of lutidine desorbed at 373 K on (a) MgP; (b) CoMo1/MgP; (c) CoMo2/MgP and (d) CoMo3/MgP.

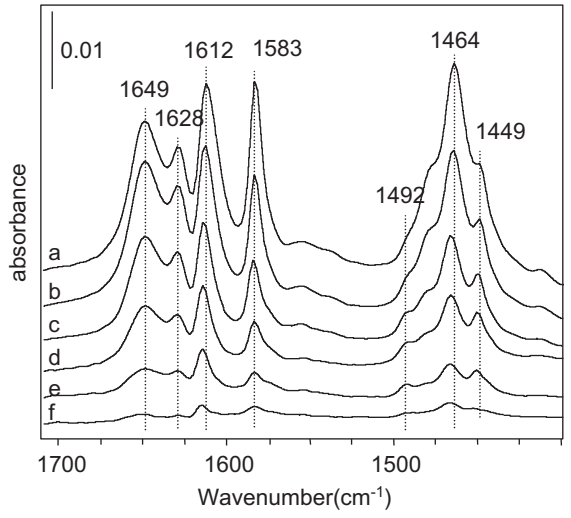

Figure 9 IR spectra of lutidine desorbed at different evacuation temperature (a) RT, (b) 323, (c) 373, (d) 423, (e) 473, (f) 523 K on CoMo1/MgP.

coordinated DMP is minimal for a catalyst containing 7.84 MoO_3 wt.% as shown Figs. 7 and 8. It appears from Fig. 9 that all the bands are maintained until 523 K evacuation temperature. It suggests that the adsorption of lutidine is not selectively adsorbed on Brönsted acid sites the contrary to that reported in literature data (Campelo et al., 1995).

3.3. X-ray photoelectron spectroscopy (XPS)

The bending energies of the Mo $3d_{5/2}$, Co $2p_{3/2}$, Mg 2p, P 2p and the XPS surface ratio for Co 2p/Mo 3d, and Mg 2p/P 2p are listed in Table 3. For comparison purposes, reference samples Mo2/MgP and Co2/MgP have been also analysed after calcination.

The Mo 3d spectrum (Fig. 10) presents the two spin–orbit components, $3d_{5/2}$ and $3d_{3/2}$ with an energy separation of 3 eV. The shape is in agreement with that reported for corresponding 3d line of bulk MoO_3 (Kim et al., 1994). The BEs of Mo 3d photopic are characteristic of the Mo(VI) species (Portela et al., 1995; Shimada et al., 1988; Koranyi et al., 1989).

The surface atomic ratios, Co 2p/Mo 3d vary with the impregnation procedure. Whereas the intensity ratio of Co2p/Mo3d (0.49) for CoMo22/MgP sample (simultaneous impregnation) is nearly equal to a theoretical ratio (0.5), indicating that the cobalt and molybdenum are dispersed homogeneously on the support surface, the solid prepared with two impregnations CoMo22/MgP has a Co/Mo ratio equal to 0.80. This latter preparation method leads to cobalt deposition over molybdenum species, with an inhomogeneous distribution.

The XPS spectra of Co 2p are shown in Fig. 10. The spectra contain, respectively, the spin–orbit components Co $2p_{3/2}$ and Co $2p_{1/2}$ at about 782 and 797.8 eV. From the photopics, spin–orbit and shake-up satellites, the peaks observed are attributed to Co^{2+} species on the catalyst surfaces (Wagner et al., 1978), present as CoO (Okamoto et al., 1980; Chin and Hercules, 1982).

3.4. 33DMB1 isomerization

The 33DMB1 isomerisation reaction was performed at a temperature between 493 and 653 K. Fig. 11 shows the conversion of MgP and CoMo/MgP catalysts for the 33DMB1 isomerisation performed at five reaction temperatures, after 4 h of reaction. All the catalysts studied are active in the 33DMB1 isomerisation. However, the behaviour of the supported catalysts differs from that of MgP because the activity of the Co–Mo catalysts present a maximum at 613 or 573 K for CoMo1 and the CoMo2, CoMo22 and CoMo3 catalysts, respectively. As seen in Fig. 11 the conversion on MgP catalyst increases with the temperature reaction increases, this suggests that MgP has the highest total number of acid sites at high reaction temperatures. This super-acidity of MgP is due to the simulta-

Table 3 The values of the binding energies (BE) of the Mo $3d_{5/2}$, Co $2p_{3/2}$, Mg 2p and P 2p photoelectrons and atomic ratios of Co 2p/Mo 3d and Mg 2p/P 2p for the catalysts.

Catalysts	Binding energies (eV)				Atomic ratios from XPS		Atomic ratios theoretical	
	Co $2p_{3/2}$	Mo $3d_{5/2}$	Mg 2p	P 2p	Co/Mo	Mg/P	Co/Mo	Mg/P
Mo2/MgP	–	232.80	50.70	133.70	–	1.42	–	1.5
Co2/MgP	782.00	–	50.70	133.60	–	1.73	–	1.5
CoMo2/MgP	782.50	232.90	50.60	133.80	0.80	1.45	0.5	1.5
CoMo22/MgP	782.00	233.00	50.70	133.70	0.49	1.48	0.5	1.5

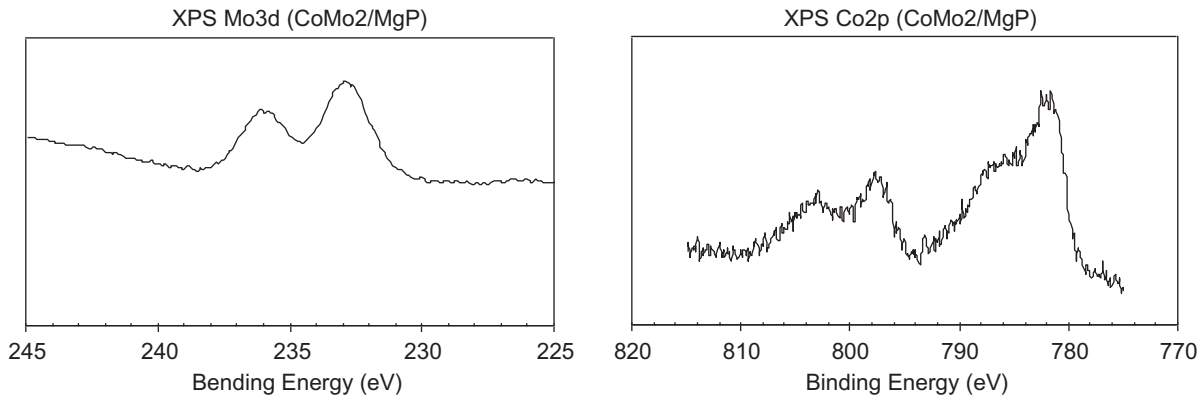

Figure 10 The Mo 3d and Co 2p spectra of the CoMo2/MgP sample calcined under air flow at 673 K.

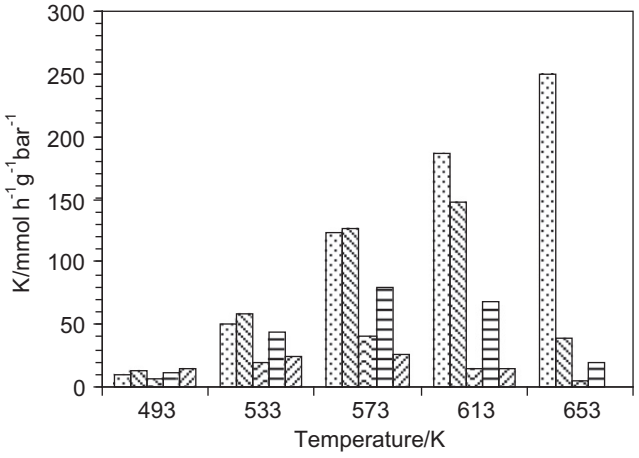

Figure 11 33DMB1 isomerization as function of the reaction temperature. Catalysts: ▨: MgP, ▨: CoMo1/MgP, ▨: CoMo2/MgP, ▤: CoMo22/MgP and ▨: CoMo3/MgP.

neous presence along with the strongest number of Lewis and Brônsted acid centres. After reaction at 573 K, methylpentenes appear as well and their formation requires relatively strong acid sites (Pines, 1982), but the conversion of 33DMB1 is decreasing on CoMo/MgP catalysts, and especially over CoMo3/MgP, which contains a high Co–Mo load. The deactivation is more pronounced with CoMo/MgP than with MgP. As seen in Fig. 12, the conversion on CoMo3/MgP is decreasing until about 50% (between the initial and final points) at 573 K and more at $T > 573$ K. This deactivation is probably due to the deposition of coke owing to other secondary reactions (Haber and Lalik 1997). The CoMo22/MgP (simultaneous impregnation) catalyst exhibits more activities than CoMo2/MgP catalyst (successive impregnation). This is due to the number of molybdenum atoms (Bronsted acid sites) found on the catalysts surface, in agreement with the XPS results observed previously.

Moreover, the 23DMB2/23DMB1 ratios for all the catalysts decrease with the reaction (pre-treatment) temperature increase as seen in Fig. 13, can be attributed to the transformation of protonic sites to Lewis sites with the elimination of the hydroxyl groups, according to literature (Burke and Ko, 1991). This ratio was greater for magnesium phos-

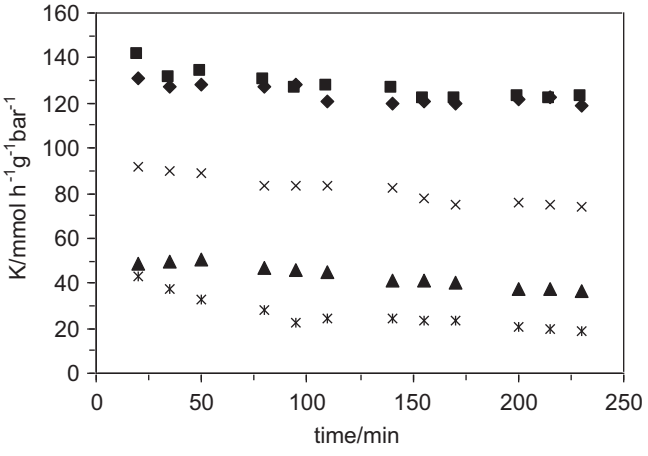

Figure 12 33DMB1 isomerization at 573 K as function of the time. Catalysts: ♦: MgP, ■: CoMo1/MgP, ▲: CoMo2/MgP, ×: CoMo22/MgP and ✳: CoMo3/MgP.

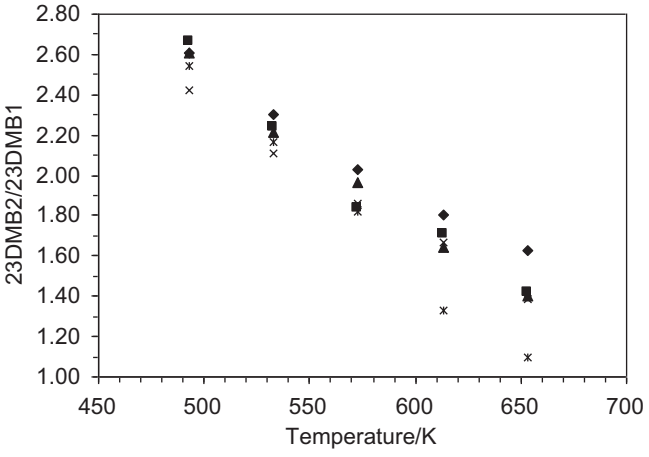

Figure 13 Change of the 23DMB2/23DMB1 ratio versus the reaction temperature. Catalysts: ♦: MgP, ■: CoMo1/MgP, ▲: CoMo2/MgP, ×: CoMo22/MgP and ✳: CoMo3/MgP.

phate than for supported oxide catalysts at high thermal treatment, that the water is more easily eliminated from oxide supported than from magnesium phosphate (Fig. 13).

The activation energies determined from the Arrhenius plots for 33DMB1 isomerisation are also given between 473 and 573 K. Obviously, the highest activation energy was obtained on MgP, and it decreased in order MgP:74 > CoMo1/MgP:66 > CoMo2/MgP ≈ CoMo22/MgP:56 > CoMo3/MgP: 18 kJ mol^{-1}. It can be presumed that the surface properties are depending on the Co–Mo oxide load. For instance, the highest content of Co–Mo phase makes easier the deposition of coke on the surface catalysts.

4. Conclusion

According to the experimental results obtained in the present work, MgP catalyst exhibited higher activity than MgP supported CoMo, in the skeletal isomerisation of 3,3-dimethyl-1-butene. Catalytic activity was strongly influenced by the impregnation method and thus, CoMo22/MgP catalyst obtained by simultaneous impregnation showed the highest conversion than those obtained by successive impregnation. This is due to high number of molybdenum atoms on the surface versus cobalt atoms. The changes in catalytic activity were related to the changes in acidic properties, which depended to Co–Mo content. The deactivation of these catalysts could be due to coke deposited on the catalyst surface during the 33DMB1 isomerisation, especially at reaction temperature > 573 K. This deactivation was increased with the Co–Mo content, thus strong acid sites of Brônsted are deactivated more quickly than weaker ones.

Acknowledgement

The authors are grateful to the Comité Mixte Interuniversitaire Franco-Marocain (CMIFM) for financial support through grant MA/02/36 and MA/06/145.

References

Aramendia, M.A., Borau, V., Jiménez, C., Marinas, J.M., Porras, A., Urbano, F.J., 1996. J. Catal. 161, 829.
Aramendia, M.A., Borau, V., Jiménez, C., Marinas, J.M., Romero, F.J., 1999. J. Colloid Interf. Sci. 217, 288.
Aramendia, M.A., Borau, V., Jiménez, C., Marinas, J.M., Romero, F.J., Urbano, F.J., 2000. J. Colloid Surf. A: Physicochem. Eng. Aspects 170, 51.
Aramendia, M.A., Borau, V., Jiménez, C., Marinas, J.M., Romero, F.J., Urbano, F.J., 2002. J. Mol. Catal. A: Chem. 182–183, 25.
Bautista, F.M., Campelo, J.M., Garcia, A., Luna, D., Marinas, J.M., Romero, A.A., Urbano, M.R., 1998. React. Kinet. Catal. Lett. 64 (1), 41.
Beebe, T.P., Gelin, P., Yates, J.T., 1984. J. Surf. Sci. 148, 526.
Boehm, H.P., Knözinger, H., 1983. In: Anderson, J.R., Boudart, M. (Eds.), Catalysis Science and Technology, vol. 4. Springer, Berlin, p. 40.
Brunauer, S., Deming, L.S., Deming, W.S., Teller, E., 1940. J. Am. Chem. Soc. 62, 1723.
Burke, P.A., Ko, E.I., 1991. J. Catal. 129, 38.
Campelo, J.M., Garcia, A., Gutiérrez, J.M., Luna, D., Marinas, J.M., 1983. J. Colloid Interf. Sci. 95, 544.
Campelo, J.M., Garcia, A., Gutiérrez, J.M., Luna, D., Marinas, J.M., 1984. J. Colloid Interf. Sci. 102, 107.
Campelo, J.M., Garcia, A., Herencia, J.F., Luna, D., Marinas, J.M., Romero, A.A., 1995. J. Catal. 151, 307.
Chin, R.L., Hercules, D.M., 1982. J. Phys. Chem. 86, 3079.
Corma, A., Rodellas, C., Fornes, V., 1984. J. Catal. 88, 374.
Florentino, A., Cartraud, P., Magnoux, P., Guisnet, M., 1992. Appl. Catal. A 89, 142.
Gallace, B., Moffat, J.B., 1982. J. Catal. 76, 182.
Guisnet, M., 1990. Acc. Chem. Res. 23, 392.
Haber, J., Lalik, E., 1997. Catal. Today 33, 119.
Haneda, M., Joubert, E., Mérézo, J.C., Duprez, D., Barbier, J., Bion, N., Daturi, M., Saussey, J., Lavalley, J.C., Hamada, H., 2001. J. Phys. Chem. Chem. Phys. 3, 1366.
Irvine, E.A., John, C.S., Kemball, C., Pearman, A.J., Day, M.A., Sampson, R.J., 1980. J. Catal. 61, 326.
Kim, D.S., Wachs, I.E., Segawa, K., 1994. J. Catal. 149, 268.
Koranyi, T.I., Manninger, I., Paal, Z., Marks, O., Gunter, J.R., 1989. J. Catal. 116, 422.
Lahousse, C., Aboulayt, A., Maugé, F., Bachelier, J., Lavalley, J.C., 1993. J. Mol. Catal. 84, 283.
Lahousse, C., Maugé, F., Bachelier, J., Lavalley, J.C., 1995. J. Chem. Soc. Faraday Trans. 91 (17), 2907.
Martin, D., Duprez, D., 1997. J. Mol. Catal. A 118, 113.
Martin, C., Martin, I., Delmoral, C., Rives, V., 1994. J. Catal. 146, 415.
Matulewicz, E.R.A., Kerkhof, F.P.J.M., Moulijin, J.A., Reitsma, H.J., 1980. J. Colloid Interf. Sci. 77, 110.
Moffat, J.B., Vetrivel, R., Viswanathan, B., 1985. J. Mol. Catal. 30, 171.
Okamoto, Y., Imanaka, T., Teranishi, S., 1980. J. Catal. 65, 448.
Paukshtis, E.A., Yurchenko, E.N., 1983. Russ. Chem. Rev. (Engl. Transl.) 52, 242.
Petit, C., Maugé, F., Lavalley, J.C., 1997. In: Froment, B.V.G.F., Delmon, B., Grange, P. (Eds.), Studies in Surface Science, vol. 106. Elsevier Science, p. 157.
Pines, H., 1982. J. Catal. 78, 1.
Portela, L., Grange, P., Delmon, B., 1995. J. Catal. 156, 254.
Rouimi, M., Ziyad, M., Leglise, J., 1999. Phosphorus Res. Bull. 10, 418.
Sadiq, M., Sahibed-dine, A., Baalala, M., Nohair, K., Bensitel, M., Lamonier, C., Peyen, E., Leglise, J., 2005. Phys. Chem. News 25, 98.
Sadiq, M., Bensitel, M., Lamonier, C., Leglise, J., 2008. Solid State Sci. 10 (4), 434.
Samantaray, S.K., Parida, K., 2001. J. Mol. Catal. A: Chem. 176, 151.
Shimada, H., Sato, T., Yoshimura, Y., Hiraishi, J., Nishijma, A., 1988. J. Catal. 110, 275.
Sing, K.S.W., Everest, D.H.R., Haul, R.A.W., Moscou, L., Pierotti, R.A., Rouquérol, J., Siemieniewska, T., 1985. Pure Appl. Chem. 57, 603.
Sokolovski, V.D., Osipova, Z.G., Plysasova, L.M., Davydov, A.A., Budneva, A.A., 1993. Appl. Catal. A: Gen. 101, 15.
Tascon, J.M.D., Grange, P., Delmon, B., 1986a. J. Catal. 97, 287.
Tascon, J.M.D., Bertrand, P., Genet, M., Delmon, B., 1986b. J. Catal. 97, 300.
Wagner, C.D., Riggs, W.M., Davis, L.E., Moulder, J.F., Mullenberg, G.E., 1978. In: Mullenberg, C.E. (Ed.), Handbook of X-ray Photoelectron Spectroscopy. Perkin–Elmer, Eden Prairie, MN.
Zaki, M.I., Knozinger, H., 1987. Mater. Chem. Phys. 17, 201.
Zaki, M.I., Hasan, M.A., Al-Sagheer, F.A., Pasupulety, L., 2000. Langmuir 16, 430.
Zhidomirov, G.M., Kazansky, V.B., 1986. Adv. Catal. 34, 131.